



Received: 03/04/2025

Accepted: 28/04/2025

Anales de Edificación

Vol. 11, Nº1, 30-41 (2025)

ISSN: 2444-1309

DOI: 10.20868/ade.2025.5509

## Datos climáticos experimentales a largo plazo para la evaluación del confort energético y térmico en el entorno construido

## Long-term experimental climate data for the energy and thermal comfort evaluation in built environment

Helena López-Moreno<sup>a,b\*</sup>; María Nuria Sánchez Egido<sup>a</sup>; Ana Amelia Navarro Fernández<sup>a</sup>; Luis F. Zarzalejo Tirado<sup>a</sup>; Emanuela Giancola<sup>a</sup>; María José Jiménez Taboada<sup>a,c</sup>; Silvia Soutullo Castro<sup>a</sup>

<sup>a</sup> Unidad de Eficiencia Energética en la Edificación, CIEMAT.

<sup>b</sup> Departamento de Construcción y Tecnología Arquitectónicas, UPM h.lopezmoreno@upm.es

<sup>c</sup> Plataforma Solar de Almería, CIEMAT

**Resumen**-- Para definir estrategias adaptadas de mitigación y adaptación al cambio climático, la metodología propuesta ofrece ventajas significativas. Este enfoque se basa en la generación de un Año Meteorológico Típico (TMYe) experimental actualizado para la ciudad de Madrid, utilizando variables meteorológicas registradas desde 2008. Además de comparar este TMYe con el ampliamente utilizado archivo climático International Weather for Energy Calculations (IWEC), se proyectaron diferentes escenarios futuros para 2050 y 2080 siguiendo trayectorias socioeconómicas compartidas. Por último, se evaluaron los indicadores de impacto a nivel climático, urbano y de edificios. Los resultados indican que tanto el TMYe como sus proyecciones revelan climas cada vez más cálidos y secos, sobre todo en verano, con temperaturas medias estivales de 32 °C y un 26% de humedad en 2080 si no se toman medidas. Esto implica un aumento sustancial de las noches tropicales, un mayor índice de incomodidad térmica y un valor significativo de los grados-hora de refrigeración, no sólo en verano, sino también en primavera y otoño.

**Palabras clave**— cambio climático; Año Meteorológico Típico (TMY); escenarios climáticos futuros; confort térmico; demanda energética.

**Abstract**— To define tailored climate change mitigation and adaptation strategies, the proposed methodology offers significant advantages. This approach is based on the generation of an updated experimental Typical Meteorological Year (TMYe) for the city of Madrid, utilizing meteorological variables recorded since 2008. In addition to comparing this TMYe with the widely used International Weather for Energy Calculations (IWEC) climate file, different future scenarios for 2050 and 2080 were projected following shared socioeconomic pathways. Finally, impact indicators at the climatic, urban, and building levels were evaluated. The results indicate that both the TMYe and its projections reveal increasingly warmer and drier climates, particularly in summer, with average summer temperatures of 32°C and 26% humidity by 2080 if no measures are taken. This implies a substantial increase in tropical nights, a higher thermal discomfort index, and a significant value of cooling degree-hours, not only in summer but also in spring and autumn.

**Index Terms**— climate change; Typical Meteorological Year (TMY); future climate scenarios; thermal comfort; energy demand.

### I. INTRODUCTION

AS the impacts of climate change intensify, particularly with the increased frequency of extreme weather events such as heatwaves, it is crucial to understand their effects on the built environment (IPCC, 2018). In Spain, the Spanish State

Meteorological Agency (AEMET) has analysed climate data from the last 40 years, highlighting that the effects directly affect more than 32 million people. These factors are evident in the expansion of semi-arid climates, the lengthening of summers (almost five weeks longer than in the early 1980s), more days of heat waves and tropical nights, and the increase in

H. L.-M., M. N. S. E., A. A. N. F., L. F. Z. T., E. G., S. S. C. are associate researchers at Unidad de Eficiencia Energética en la Edificación, CIEMAT. H. L.-M. is also associate researcher at the Departamento de Construcción y

Tecnología Arquitectónicas, UPM. M. J. J. T. is associate researcher at both the Unidad de Eficiencia Energética en la Edificación, CIEMAT and the Plataforma Solar de Almería, CIEMAT.

the Mediterranean surface temperature of  $0.34^{\circ}\text{C}$  per decade (AEMET, 2023). This situation has a significant impact on the country's economic drivers, such as large cities, making them particularly vulnerable to climate change (MITECO, 2020). Furthermore, at a global level, urban areas, despite occupying only 3% of the planet's surface are home to 55% of the population and are responsible for 67% of the global energy consumed (International Energy Agency, 2017) (*Database - Eurostat*, n.d.), with forecasts indicating an increase in the population in cities to 68% by 2050 (World Urbanization Prospects).

On the other hand, the consequences of global warming are significantly exacerbated in urban areas, which frequently experience the urban climate effect. This phenomenon leads to considerably higher temperatures and solar radiation in urban centers compared to surrounding rural areas, while humidity and wind speed are reduced. Such conditions contribute to more intense and frequent heatwaves (Palme & Salvati, 2021). These emerging climatic trends are shifting energy consumption patterns, causing a clear increase in cooling demands (OrtizBeviá et al., 2012; Soutullo et al., 2020). Indeed, in Europe, the implementation of space cooling systems, particularly in residential sectors, have demonstrated a high growth in the last years. This trend can strain an already uncertain electrical grid, influenced by factors such as evolving climate patterns and the rise of electric mobility (Kan et al., 2021). However, the widespread adoption of these cooling systems, beyond not being accessible to low-income populations, also contributes to increased ambient temperatures due to their outdoor condensation units. Furthermore, this situation could lead to higher greenhouse gas emissions if the energy is sourced from non-renewable options, perpetuating the cycle of climate change (De Munck et al., 2013).

Beyond merely considering buildings' energy demands, these impacts extend to broad aspects concerning individuals' mental and physical health (IPCC, 2021; López-Bueno et al., 2020; Xu et al., 2016). Besides, the combination of high temperatures and increased levels of air pollutants, such as ozone and PM<sub>10</sub>, commonly found in urban areas, further amplifies the risks associated with heat stress during warm seasons (Eurowho, 2021; Scortichini et al., 2018). This disproportionately affects vulnerable populations, including the elderly, individuals with chronic or mental illnesses, low-income socioeconomic groups, and workers performing manual or physical tasks (ILO, 2019; Weir, 2002). In this regard, studying thermal comfort, both indoors and in outdoor environments, is crucial for defining prevention plans aligned with climate projections (López-Bueno et al., 2020; MSSSI, n.d.). Moreover, urban and building characteristics play a critical role in this aspect (López-Moreno et al., 2020, 2021, 2022).

The urgency of addressing this situation is underscored by the Intergovernmental Panel on Climate Change (IPCC), which highlights, among the key risks for Europe, human stress and mortality due to rising temperatures and heat extremes (IPCC, 2021). However, urban energy modelling often fails to adequately incorporate this evolving climatic reality (Burillo et

al., 2019). Widely used tools and normative data sources rely on climate data that may not reflect current climate trends (Herrera et al., 2017; Sánchez et al., 2020). In Spain, data provided by EnergyPlus (IWEC and SWEC), as well as normative data defined by the Technical Building Code (MET), were last updated in 2013 (with the exception of the Canary Islands' climate zones) (CTE, 2015; EnergyPlus, n.d.). Furthermore, these climate sources, often derived from non-urban environments such as airports, omit the crucial influence of city morphology on building energy dynamics (Bianchi & Smith, 2019).

In climate change mitigation and adaptation strategies, it is important to consider not only the effects of the current climate but also those that account for future climate projections. In this regard, the IPCC, in its fifth assessment report, defined the Representative Concentration Pathways (RCPs) (Meyer, 2014). These RCPs were introduced as trajectories used to model and project future climate changes based on different levels of greenhouse gas emissions and other climatic radiative forcing. Following this idea, various studies point to the need for energy rehabilitation plans to address the growing cooling demand and overheating risks, which will be more severe in these future climate scenarios (Elnagar et al., 2023; Pérez-Andreu et al., 2018). By 2085, Spain is projected to experience a significant shift in energy demands, with heating requirements decreasing by approximately 50% under the RCP 4.5 scenario and 70% under RCP 8.5. Conversely, cooling demands for these same projections are anticipated to increase substantially, by up to 130% and 180% respectively. This trend is expected to be particularly pronounced in inland areas, such as Madrid (Amin et al., 2023; Díaz-López et al., 2021; Gangoellés & Casals, 2012). More recently, the IPCC included the Shared Socioeconomic Pathways (SSPs) in its sixth report. SSPs not only focus on climatic variations but also combine climate evolution with potential socioeconomic changes (variations in population, economy, technology, policy, and development) to explore how these factors interact and affect future human-induced climate change scenarios (IPCC, 2021).

This climatic mismatch, both present and future, reduces the ability of models to accurately predict energy needs and comfort conditions in the context of a changing climate. Climate monitoring campaigns are presented as key instruments for evaluating the behaviour of buildings and their components (Sirombo et al., 2017). To address this limitation, the present study aims to characterize the impact that the current climate can have on building energy analysis and thermal comfort, as well as the implications of future climate change scenarios. For this purpose, the use of updated experimental climate data, collected over more than a decade (2008-2021) at the CIEMAT headquarters in Moncloa (Madrid), has been proposed (Olmedo et al., 2016; Sánchez et al., 2020). The meteorological variables from these experimental data have been processed to create a Typical Meteorological Year (TMY) according to UNE-EN ISO-15927-4:201 (AENOR, 2011). Subsequently, the analysis involves a comparative evaluation between widely used climate data files for building energy simulation programs, such as

IWEC, with current experimental climate data (TMYe) and their possible future climate trends through SSP scenarios. Finally, for a better understanding of climatic impacts on the built environment, this methodology analyses different climatic, urban, and building indicators.

The proposed work enables an estimation of future climate trends, as well as their comfort and building energy implications, facilitating responsible climate design and sustainable urban development.

## II. METHODS

To assess the impact of different climate scenarios on thermal comfort and building energy consumption, this study analyses various indicators at the climatic, urban, and building levels. The methodology involves processing over 10 years of experimental campaign data to define an updated Typical Meteorological Year (TMY). This updated TMY will then be compared with the International Weather for Energy Calculations (IWEC) file from EnergyPlus software. Furthermore, the study will examine future projections for both the TMY and IWEC files, based on Shared Socioeconomic Pathways (SSPs) for 2050 and 2080.

The chosen case study is the city of Madrid, an urban environment home to over 3 million people of great socioeconomic diversity and one of Spain's primary economic drivers. Its inland location and climate are key factors in addressing climate change (Giannakopoulos et al., 2009).

### A. Definition of Typical Meteorological Years.

According to the Köppen-Geiger climate classification, Madrid has a Mediterranean climate (Csa), characterized by warm temperatures with mild and cool winters, while summers are hot and dry, with these conditions exacerbated by the urban microclimate (Beck et al., 2018).

For Madrid, CIEMAT has developed an experimental methodology to evaluate current climatic trends. This methodology is based on long-term meteorological monitoring (from 2008 to 2021) at its Moncloa facilities in Madrid (Sánchez et al., 2020). These data, recorded at minute frequency, have been processed to generate a precise and reliable multi-year climate database. This involved extensive filtering and treatment of key meteorological variables, such as air temperature (Ta), relative humidity (RH), horizontal global solar radiation (Gh), and wind velocity (Wv). The climate sensors consist of two meteorological stations that simultaneously record data from the same location, with the second station complementing the first to avoid potential data gaps.

Subsequently, using this climate database, an experimental Typical Meteorological Year (TMYe) was created following the criteria of UNE-EN ISO-15927-4:2011. This standard defines the creation of a TMY for evaluating the average annual energy for heating and cooling, based on concatenating the twelve representative typical meteorological months: the "best" January, the "best" February, March, etc. To achieve this, each variable (Ta, RH, Gh, and Wv) is analysed separately, and those months whose daily average values are closest to the cycle's

average are selected. This process involves calculating Cumulative Distribution Functions (CDFs) and subsequently applying the Finkelstein-Schafer (FS) statistic (Finkelstein & Schafer, 1971) for Ta, RH, and Gh. Additionally, UNE 15927-4 defines the contribution of different climatic parameters to the TMY selection through weighting factors ( $w_i$ ) that balance their influence. The three candidate months will be those with the lowest FS sum ( $FS_{sum}$ ) (Equation 1) [41]. In this study, following the criterion of T. Kalames et al., the parameters Ta, RH, and Gh were weighted equally ( $w_i = 1/3$ ) (Kalamees et al., 2012). Finally, considering only the three previously selected candidate months, the finalist months comprising the TMY will be those with the smallest deviation in the Wv variable between the daily means and the cycle's mean.

$$FS_{sum} = w_1 FS(Ta) + w_2 FS(RH) + w_3 FS(Gh) \quad (\text{Eq. 1})$$

For comparison with other databases, the IWEC (International Weather for Energy Calculations) climate file for Madrid, provided by the EnergyPlus software, was used. Similarly, these files, defined by ASHRAE using hourly meteorological data recorded between 1982 and 1999, were synthetically generated for use with building energy simulation programs by creating a "typical" climate year. Comparing both climate files (the updated TMYe and IWEC) allows for an assessment of climatic evolution and its impacts.

### B. Shared Socioeconomic Pathways (SSPs)

The Shared Socioeconomic Pathways (SSPs), introduced in the IPCC's Sixth Assessment Report (AR6), enable professionals to explore climate changes under different future scenarios, which are essential for climate adaptation policies and strategies. They are based on the results of Global Climate Models (GCMs) and their coupling through the sixth phase of the Coupled Model Intercomparison Project (CMIP6). SSPs were developed to complement the Representative Concentration Pathways (RCPs), generated under the previous modelling phase (CMIP5), by incorporating diverse socioeconomic challenges for adaptation and mitigation. Therefore, unlike RCPs, SSP scenarios describe the human factors influencing greenhouse gas (GHG) emissions and radiative forcing (the additional energy trapped in the climate system due to GHGs). Furthermore, they standardize socioeconomic characteristics that affect GHG emissions, indicating social trajectories associated with different warming levels. They also allow for the evaluation of the effectiveness of actions to comply with the Paris Agreement, limiting the global temperature increase to less than 2°C (SSP1-1.9) (IPCC, 2022). SSPs are classified into five "families" based on two axes: challenges for mitigation and challenges for adaptation. SSP1 (Sustainability) presents few challenges for both mitigation and adaptation, while SSP3 (Regional Rivalry) faces significant challenges for both. The other SSPs complete the spectrum of possible futures: SSP4 (Inequality) has high adaptation challenges and low mitigation challenges, SSP5 (Fossil-fueled Development) has high mitigation challenges and low adaptation challenges, and SSP2 (Middle of the Road) represents moderate challenges for both.

Considering this concept, the present methodology analyses,

for both the TMYe and EPW climate files, the SSP scenarios projected for 2050 and 2080. For this purpose, the Future Weather Generator tool was utilized (Rodrigues et al., 2023). This tool is based on the "morphing" method, which involves mathematically transforming the current climate to match the projected variables of a climate change scenario. These are calculated from numerical models provided by GCMs, which represent physical processes in the atmosphere, ocean, cryosphere, and land surface, using CMIP models as a reference. Compared to similar tools that employ this "morphing" mathematical adjustment, Future Weather Generator was selected for its greater advantages, including its open-source nature and updated GCM models (based on CMIP6, which includes EC-Earth3 among others), providing recent baseline data and future projections, as well as higher spatial resolution. Specifically, the SSPs defined by Future Weather Generator are:

- SSP1-2.6: Sustainability, "Green Road": Global CO<sub>2</sub> emissions are drastically reduced, reaching net zero after 2050. Temperatures stabilize at around 1.8 °C higher by the end of the century.
- SSP2-4.5: "Middle of the Road": Global CO<sub>2</sub> emissions will not reach net zero by 2100. Temperatures will increase by 2.7 °C by the end of the century.
- SSP3-7.0: Regional Rivalry, "Rocky Road": Global CO<sub>2</sub> emissions will approximately double from current levels by 2100. By the end of the century, average temperatures will have increased by 3.6 °C.
- SSP5-8.5: Fossil-fueled Development, "Taking the Highway": Current CO<sub>2</sub> emission levels will approximately double by 2050. By 2100, the global average temperature will increase to 4.4 °C.

This tool requires climate files in EnergyPlus Weather file (.epw) format. Therefore, the TMYe climate file was converted to this format using EnergyPlus's "Weather Statistics and Conversions" software (Programs, 2022).

### C. Analysis of Climate Change Impact

Based on these SSP projections, their potential impacts at the climatic, urban, and building levels have been studied using various indicators related to climate change, human health, and energy demand. To achieve this, different indices have been analysed, combining the various base climates (TMYe and IWEC) and SSP scenarios (SSP1-2.6, SSP2-4.5, SSP3-7.0, and SSP5-8.5), as well as their projections for 2050 and 2080.

At the climatic level, this evaluation was conducted using the climate indices defined in the European Climate Assessment & Dataset Project (ECA&D), which allow for the quantification and harmonization of historical, present, and future climate trends [46]. Due to their relevance to this study, the following indicators have been defined:

- Extreme Temperature Range (ETR): Provides information on extreme temperature variability in a given area. Its calculation is established by the difference between the daily maximum and minimum temperatures for a specific period.

- Tropical Nights (TR): Used to evaluate the impact of climate change on night-time temperatures. It is defined as the number of nights in a specific period (usually a year) where the minimum temperature does not drop below 20°C.
- Summer Days (SU): Analyses extreme heat conditions during summer. It is defined as the number of days in a given period where the daily maximum temperature exceeds 25°C.
- Frost Days (FD): Defines extreme cold conditions. It is calculated by counting the number of days where the daily minimum temperature is below 0°C in a given period.

At the urban level, outdoor thermal comfort has been studied, as it is of great importance for urban planning, architectural design, landscape design, transportation, tourism, and urban health, among others. ASHRAE defines thermal comfort as the mental condition that expresses satisfaction with the thermal environment (ASHRAE, 2017). Outdoor thermal comfort is a complex concept affected by many factors, including the environment, the individual, and psychology (Lai et al., 2020). Among these, environmental factors such as radiation, wind, temperature, and humidity directly affect the human body's thermal balance and sensation (Reiter, 2004). Empirical thermal comfort assessment indices offer a simpler and more understandable calculation method compared to theoretical thermal comfort assessment indices. Although they have limitations in considering human physiology, they are frequently used in the early stages of comfort studies. Among the most common empirical methodologies for studying heat stress are the Heat Stress Index (HSI), the Wet Bulb Globe Temperature Index (WBGT), the Heat Index (HI), and the Discomfort Index (DI) (Liu et al., 2023).

The Discomfort Index (DI), proposed by Thom in 1959 and used to evaluate the level of thermal discomfort perceived by people due to environmental conditions through effective temperature, was selected (Liu et al., 2023; Thom, 1959). This index is characterized by its simplicity of evaluation, which facilitates its calculation compared to other methods (Tselepidaki et al., 1992). It relates dry bulb temperature and relative humidity using the following formula (Equation 2):

$$DI = T - (0.55 - 0.0055 \times RH) \times (T - 14.5) \quad (\text{Eq. 2})$$

Where  $T$  is the dry bulb temperature in degrees Celsius and  $RH$  is the relative humidity in percentage. Based on these values, intensity limits are established to facilitate the interpretation of this value:

- Intensity 0:  $DI < 21$ : Comfort.
- Intensity 1:  $21 \leq DI < 24$ : Less than half of the population feels thermal discomfort.
- Intensity 2:  $24 \leq DI < 27$ : More than half of the population feels thermal discomfort.
- Intensity 3:  $27 \leq DI < 29$ : Most of the population feels thermal discomfort.
- Intensity 4:  $29 \leq DI < 32$ : Everyone feels severe heat stress.
- Intensity 5:  $> 32$ : Medical emergency state.

Finally, at the building level, degree-days calculations have

been used to estimate the potential heating and cooling demands of buildings under climate change scenarios. This method quantifies the accumulation of heat or cold over time by calculating the differences between the measured temperature and a reference threshold over a specific period (Martinopoulos et al., 2019). The Regulation of Thermal Installations in Buildings (RITE, RD 1027/2007) in Spain defines design limits of 23-25°C for summer and 21-23°C for winter (BOE 15820, 2007). Furthermore, the recent RD 14/2022 regulation, focused on defining various measures including those aimed at energy saving, energy efficiency, and reducing natural gas energy dependence, limits heating and cooling temperatures to 19°C and 27°C, respectively (BOE 12925, 2022). Using RD 14/2022 as a reference, which is more aligned with current climate challenges, heating degree-hours (HDD) have been calculated for accumulated degrees below 19°C, while cooling degree-hours (CDD) have been quantified as those above 27°C.

### III. RESULTS

Building upon the methodology described in the previous section, the following subsections present the climatic results for the updated experimental Typical Meteorological Year (TMYe), generated according to UNE 15927-4, and its Shared Socioeconomic Pathways (SSP) scenarios for 2050 and 2080. Additionally, the results of the climatic impact indices (ETR, FD, SU and TR), the urban impact index (DI), and the building impact indices (HDD and CDD) are described.

#### A. Experimental Typical Meteorological Year (TMYe) and its Future SSP Scenarios

This section presents data derived from Madrid's experimental Typical Meteorological Year (TMYe), calculated using CIEMAT's climate database and the UNE 15927-4 standard. Hourly data for the main meteorological variables are displayed through box-and-whisker plots (boxplots), which allow for the identification of interquartile ranges (Q2 and Q3 via the box, Q1 and Q4 for the whiskers), dispersion, symmetry, mean value (crosses), median (horizontal line), and outliers (points). To facilitate result comparison, values from the IWEC climate file, TMYe, and TMYe projections for the "Green Road" (SSP1-2.6), "Middle of the Road" (SSP2-4.5), "Rocky Road" (SSP3-7.0), and "Taking the Highway" (SSP5-8.5) scenarios for 2050 (top) and 2080 (bottom) have been jointly plotted. These results are presented at an annual level (right) and disaggregated seasonally (left), enabling a detailed study of interannual variations.

##### 1) Outdoor Air Temperature ( $T_a$ )

**Error! Reference source not found.** presents the results for the air temperature ( $T_a$ ) variable. Comparing the current IWEC results with the experimental TMYe, it is observed that TMYe presents warmer annual mean temperature values (16.0°C) compared to IWEC (14.3°C). This behaviour is consistent at the seasonal level, with mean winter values of 7.2°C and 8.7°C and summer values of 25.8°C and 24.0°C for TMYe and IWEC, respectively. Minimum hourly values reach around -3.7°C and maximums around 40°C for both cases.

Analysing the TMYe projections, we observe that as

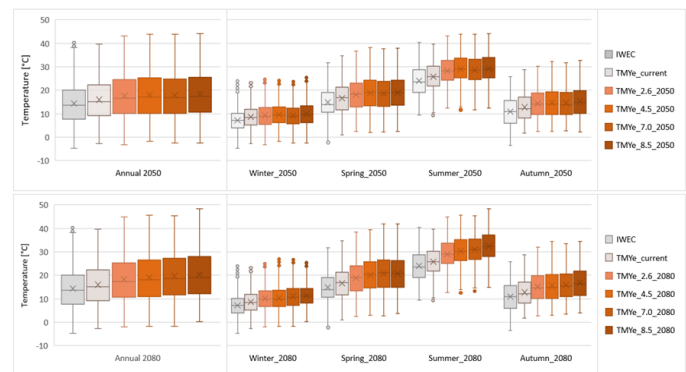


Fig. 1. Air Temperature ( $T_a$ ) of IWEC, TMYe climates and their SSP1-2.6, SSP2-4.5, SSP3-7.0 and SSP5-8.5 projections for 2050 and 2080 aggregated annually and seasonally.

adaptation and mitigation challenges increase, the temperature rises, with this behaviour becoming more pronounced over time. For the year 2050, annual temperature variations between these scenarios are clearly higher than TMYe, with annual mean values ranging from 17.6°C for SSP1 to 18.4°C for SSP5, showing similar interquartile ranges for all SSPs. In the analysis of the 2080 projection, these differences are much more noticeable, with annual mean values ranging from 18.4°C for SSP1 to 20.4°C for SSP5. Furthermore, in this case, the interquartile ranges do increase in temperature as the SSPs present higher levels of inaction and inequality. Performing this analysis at a seasonal level, we can observe slight increases in mean temperatures during winter months, with temperatures of 9.3°C for SSP1 and 9.9°C for SSP5 in 2050 ( $\Delta T_a$  of 0.6°C and 1.2°C). In 2080 these figures increase from 10.2°C to 11.4°C for SSP1 and SSP5, respectively ( $\Delta T_a$  of 1.4°C and 2.7°C). This trend gradually increases in autumn and spring. Finally, in the summer months, the mean temperature values are significantly higher. Specifically, during summer, mean temperature values are 28.3°C for SSP1 and 29.3°C for SSP5 in 2050 ( $\Delta T_a$  of 2.6°C and 3.5°C relative to TMYe), while in 2080 these figures increase from 29.1°C to 32.4°C for SSP1 and SSP5, respectively, representing a  $\Delta T_a$  of 3.3°C and 6.7°C relative to TMYe. Moreover, under the SSP5 scenario, extreme temperatures could reach 44.2°C in 2050 and 48.5°C in 2080.

##### 2) Relative Humidity (RH)

Figure 3 illustrates the results for relative humidity (RH). In this case, IWEC shows higher annual mean humidity values of 62%, compared to TMYe's mean of 53%. Seasonally, RH follows the same trend, with mean values of 70% and 62% in winter and 45% and 33% in summer for IWEC and TMYe, respectively. Maximum hourly values reach 100%, while minimums can drop to 12% for IWEC and 5% for TMYe.

Focusing on the comparison of TMYe with its climate projections, a slight reduction in humidity is observed as scenarios evolve from SSP1 to SSP5, becoming somewhat more evident over time. For 2050, variations in relative humidity are minor, with annual mean values ranging from 53% for SSP1 to 50% for SSP5, and very similar interquartile values. Similarly, for 2080, annual mean RH shows ranges between 51% for SSP1 and 49% for SSP5, with similar interquartile ranges. Seasonally disaggregating these data, the highest figures are found in winter, around 63%, with very similar RH

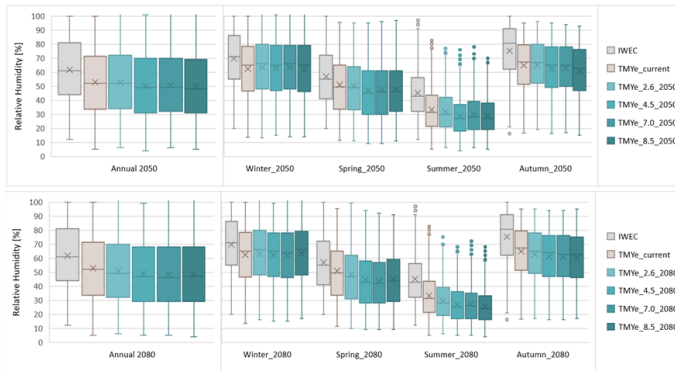


Fig. 2. Relative Humidity (RH) of IWEC, TMYe climates and their SSP1-2.6, SSP2-4.5, SSP3-7.0 and SSP5-8.5 projections for 2050 and 2080 aggregated annually and seasonally.

for all SSPs and years, practically identical to the current TMYe ( $\Delta RH$  of 1%). This is followed by the RH values in autumn and spring. Conversely, summer exhibits the lowest values, where differences are more noticeable. RH for 2050 is 32% in SSP1 and 29% in SSP5 ( $\Delta RH$  of 1% and 4% relative to TMYe), while in 2080, observed variations range from 30% to 26% for SSP1 and SSP5, respectively ( $\Delta RH$  of 3% and 7% relative to TMYe). The maximum and minimum hourly RH values are very similar across all SSPs and years, reaching 100% in winter, while in summer; the hourly minimums are around 5%, both figures practically identical to TMYe.

### 3) Global Horizontal Solar Radiation (Gh)

Figure 4 displays the daily global horizontal solar radiation (Gh) values. Values above 10 W/m<sup>2</sup> were used as reference, ensuring a minimum solar height. The values recorded by TMYe and IWEC are very similar, with annual mean values of 386 and 379 W/m<sup>2</sup> respectively. In both cases, maximum figures are reached in summer (490 W/m<sup>2</sup> seasonal average), very close to values recorded in spring (437 W/m<sup>2</sup> seasonal average), where daily maximums approach 1100 W/m<sup>2</sup>. In winter, the average seasonal radiation reduces to 280 W/m<sup>2</sup>, while in autumn; the minimum values are reached, averaging 262 W/m<sup>2</sup>. Analysing the TMYe climate projections, a very slight increase in solar radiation can be observed, with hardly any variations found between the SSP scenarios and the years 2050 and 2080. Annually, the means for all SSPs and years are 405 W/m<sup>2</sup>. Following the same previous trend, the summer season presents the highest mean values (511 W/m<sup>2</sup>), followed by the figures shown in spring, where daily maximums are close to 1200 W/m<sup>2</sup>. Finally, in autumn, the average seasonal value decreases to 285 W/m<sup>2</sup>.

### 4) Wind Velocity (Wv)

Figure 5 describes the wind velocity (Wv). The annual mean values for TMYe (1.39 m/s) are lower than those for IWEC (2.44 m/s). In autumn, both show the lowest values: 1.38 m/s for TMYe and 1.15 m/s for IWEC. Maximum values vary seasonally, with the highest mean values recorded in spring for TMYe (1.60 m/s) and in winter for IWEC. The SSP projections are similar to TMYe, with slight differences in the SSP5 scenario, especially in autumn, with mean minimums of 1.1 m/s.

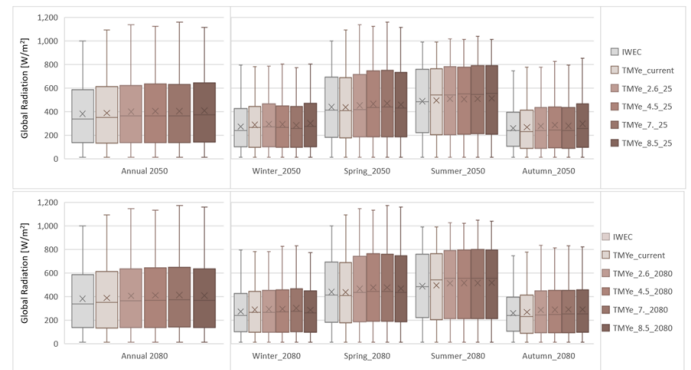


Fig. 3. Global Horizontal Solar Radiation (Gh) of IWEC, TMYe climates and their SSP1-2.6, SSP2-4.5, SSP3-7.0 and SSP5-8.5 projections for 2050 and 2080 aggregated annually and seasonally.

## B. Climatic, Urban, and Building Impact Indicators

This section presents the results obtained from the study of each selected indicator used to evaluate the impact of the current climate and its SSP projections.

### 1) Climatic Indicators: Meteorological Variable Trends.

Following the methodology defined by the ECA&D, Figure 6 illustrates the climatic indices ETR, FD, SU, and TR for the IWEC and TMYe climate files and their SSP1-2.6, SSP2-4.5, SSP3-7.0, and SSP5-8.5 projections for 2050 (top) and 2080 (bottom).

For the ETR indicator, values provided by IWEC are considerably higher than the experimental TMYe values, with differences of 22.8°C compared to 19.0°C, respectively. Analysis of ETR for the TMYe's SSP scenarios reveals that the extreme temperature range increases as the SSPs present greater challenges, reaching 19.5°C in SSP5 by 2050. This trend intensifies in the 2080 projection, peaking at 20.5°C in SSP3, where it appears to begin a decline in SSP5.

Regarding the TR indicator, significant differences are observed when comparing the 12 TRs of IWEC with the 41 obtained for TMYe. Examining this behaviour across different SSPs, these figures increase from 75 to 88 TR for SSP1 and SSP5 in 2050, respectively, and further to 83 and 108 for SSP1 and SSP5 in 2080. Notably, these increases in 2080 are largely due to the rise in TR primarily in spring, but also in autumn (totalling 26 TR for SSP5 in 2080).

Conversely, the number of SU for current climates is similar, being slightly higher for TMYe with 125 days compared to

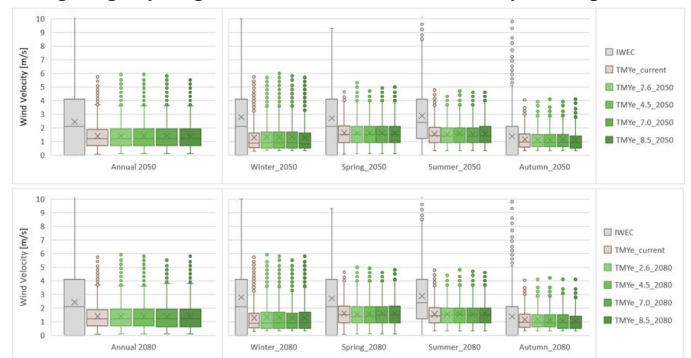


Fig. 4. Wind Velocity (Wv) of IWEC, TMYe climates and their SSP1-2.6, SSP2-4.5, SSP3-7.0 and SSP5-8.5 projections for 2050 and 2080 aggregated annually and seasonally.

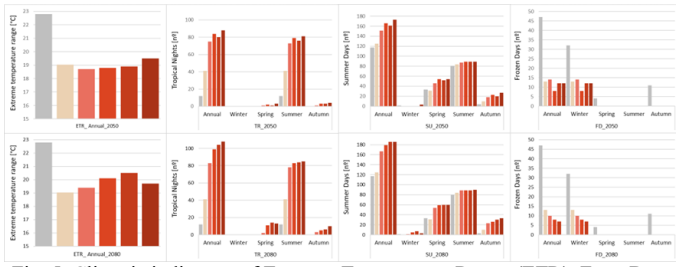


Fig. 5. Climatic indicators of Extreme Temperature Range (ETR), Frost Days (FD), Summer Days (SU), and Tropical Nights (TR) for IWEC, TMYe climate files and their SSP1-2.6, SSP2-4.5, SSP3-7.0, and SSP5-8.5 projections for 2050 (top) and 2080 (bottom).

IWEC's 117 days. In addition to SUs occurring almost throughout the summer period, summer days are also observed in spring and autumn. The SSP trends show significantly higher annual numbers compared to TMYe, with figures of 151 and 173 for SSP1 and SSP5, respectively, in 2050, increasing to 167 for SSP1 and 186 for SSP5 in 2080. For these future scenarios, SUs also cover practically the entire summer period (90 days), and the notably high number of summer days during spring and autumn is significant. In the 2050 projections, SU values are around 50 days in spring and 20 in autumn. In 2080, these values would increase to close to 60 in spring and 30 in autumn, with even a slight occurrence of summer days in winter.

Finally, for the analysis of FD, the IWEC climate file shows very high values compared to the experimental file. Annually, the FD indicator is 47 days for IWEC, with frost days found primarily in winter, but also in spring and autumn. However, the TMYe file only presents 13 FD in winter, significantly lower than IWEC. Similar to TMYe, the SSP projections only show FD values in winter. In 2050, these figures are very similar to TMYe, while in 2080, they decrease to a minimum of 7 FD for SSP5.

## 2) Urban Indicator: Outdoor Thermal Comfort

The potential impact of climate change at the urban level has been quantified using the Discomfort Index (DI). Figure 7 presents these results, expressing the percentage of hours in comfort or heat discomfort, specifying different intensities.

The TMYe climate file shows slightly higher values of outdoor heat discomfort compared to the IWEC climate, with annual values of 17% and 14%, respectively. Disaggregating these data seasonally, these figures intensify significantly in summer, reaching heat discomfort percentages of 47% for IWEC and 57% for TMYe. Various intensities of thermal discomfort are observed: Intensity 1, less than half of the population experiences heat discomfort (28% and 41% for IWEC and TMYe, respectively); Intensity 2, more than half of the population experiences heat discomfort (around 18% in both cases); and even percentages of Intensity 3, where most of the population feels heat stress. It is worth noting that values close to 10% thermal discomfort are also observed for both climates in spring.

When examining the TMYe's SSP climate trends, increases in thermal discomfort percentages are observed, ranging from 25% to 28% in 2050 and from 27% to 35% in 2080. It is important to mention that these figures for thermal discomfort increase notably in summer, reaching values around 75% in 2050 and even 91% in 2080 for SSP5. This discomfort presents

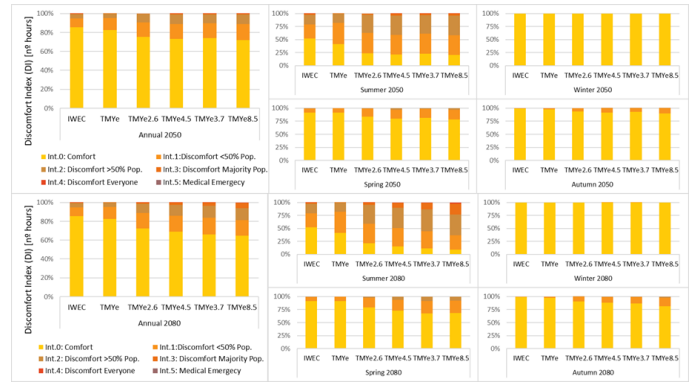


Fig. 6. Values of the urban outdoor thermal comfort indicator Discomfort Index (DI) for IWEC, TMYe climate files and their SSP1-2.6, SSP2-4.5, SSP3-7.0, and SSP5-8.5 projections for 2050 (top) and 2080 (bottom).

different intensities according to its classification: for 2050, the percentages where less than half of the population experiences heat discomfort (Intensity 1), as well as where more than half of the population experiences heat discomfort (Intensity 2), are close to 40%, showing slight values where most of the population would feel heat stress (Intensity 3). However, in 2080, the comfort percentages for TMYe's SSPs decrease drastically, with minimums in SSP5 of 9%. In this case, the percentage of hours where most of the population experiences heat discomfort (Intensity 3) is clearly higher, with ranges from 4% to 21% for SSP1 and SSP5, respectively. Although minimal, there are even instances where everyone experiences discomfort (Intensity 4).

Given these future projections, it should be highlighted that this thermal discomfort is also present in spring and autumn, with average values for 2050 of 17% and 7% respectively. This situation becomes more acute in 2080, with these figures increasing to 22% in spring, where percentages where most of the population would feel heat stress (Intensity 3) are also present, and 12% for the autumn period.

## 3) Building Indicator: Energy Demand.

Finally, this section aims to estimate the intensity of building energy demands. Figure 8 shows the heating degree-hours (HDD) and cooling degree-hours (CDD), where annually, significantly higher HDD values are observed compared to CDD. In the comparison of current climates, this proportion is 94% HDD versus 6% CDD. Specifically, the HDD value is approximately 10000°C higher for IWEC (56405°C) compared to TMYe (46470°C), while the CDD value is about 800°C lower for IWEC (3226°C) compared to TMYe (4647°C). Seasonally, disaggregating these values, it is observed that almost all CDD occur in summer.

Evaluating future SSP climate trends for TMYe reveals a shift: as SSPs present greater challenges, heating demands decrease while cooling demands increase. For 2050, the HDD-CDD proportion drops from 85-15% in SSP1 to 80-20% in SSP5. This trend becomes more pronounced in 2080, with SSP1 at 81-19% and SSP5 reaching 66-34%.

Specifically, for 2050, the HDD indicator decreases from 40350°C to 37567°C for SSP1 and SSP5 respectively (approximately 13% less than TMYe). Conversely, CDD would increase from 7360°C in SSP1 to 9146°C in SSP5, 180% and 225% more than for TMYe. In this instance, part of this increase



Fig. 7. Values of heating degree-hours (HDD) and cooling degree-hours (CDD) for IWEC, TMYe climate files and their SSP1-2.6, SSP2-4.5, SSP3-7.0, and SSP5-8.5 projections for 2050 (right) and 2080 (left).

in CDD is due not only to the values found in summer but also in spring, accounting for almost 8% of the annual CDD. For 2080, HDD would range from 37118°C to 30561°C in SSP1 and SSP5 respectively. The CDD value, however, would reach up to 8848°C in SSP1 and 15686°C in SSP5, implying an increase of 336% compared to the current TMYe. In this case, the annual contribution to the annual CDD indicator from spring data is 11%.

### C. Discussion of results

Given current climatic trends, it is crucial to define validated models that enable the projection of future scenarios to establish effective adaptation and mitigation strategies. In this regard, the proposed methodology offers significant value by providing experimental data of key meteorological variables for the city of Madrid since 2008. Notably, it includes radiation and wind data, which, despite being crucial for climate definition, are not as frequently recorded. Pyranometers and anemometers are delicate, costly instruments, and their proper placement and calibration present significant technical and operational challenges (WMO-No. 8, 2012). This climate database has allowed for the generation of an experimental Typical Meteorological Year (TMYe) according to UNE-15927-4:2011, utilizing more recent records than those used for the IWEC climate file. This is highly relevant for capturing climatic trends of the last decade. This evidence is seen in the comparison of TMYe with the reference IWEC climate file, where IWEC shows  $T_a$  values that are 1.7°C lower, while RH figures are 9 points higher. This climatic trend, characterized by higher temperatures and drier environments, aligns with climate evolution studies and the microclimatic modifications observed in urban settings (Castro Medina et al., 2024; López-Moreno et al., 2020).

However, the proposed methodology might have some limitations in recording extreme climatic events. Firstly, the TMY method, used to define both IWEC and TMYe files, relies on selecting months closest to the average of the studied series. Additionally, the meteorological stations used for generating the experimental climate database are located in an area with low building density compared to other parts of the city. Consequently, for extreme climatic situations like droughts or heatwaves, which are predicted to be more frequent, intense, and prolonged, as well as in urban areas with higher building density, the obtained results might be altered. Specifically,  $T_a$  and  $G_h$  values would be higher, while RH and  $W_v$  would

decrease, exacerbating the results obtained in the analysis of climatic, urban, and building indicators.

Another possible limitation is related to the climatic definition of future scenarios. Firstly, the "morphing" mathematical model might underestimate the increasing severity of extreme weather and its frequency, or it might not guarantee the consistency of the relationship between some climatic variables. However, for studying building energy performance or long-term thermal comfort, as in the present study, this restriction would not be as evident (Eames et al., 2012; Jentsch et al., 2013). Conversely, this model offers a computationally efficient solution, providing hourly climate data without the need for simulation adjustment (bias correction) and with less spatial and temporal data. Furthermore, despite the complexity of the CMIP6 model, SSPs still simplify many aspects of socioeconomic, political, and climate change development, which can lead to an incomplete representation of reality and long-term uncertainties. Nevertheless, the CMIP6 calculation engine is currently the best available toolset for understanding and projecting changes in the climate system (IPCC, 2021).

From the perspective of the variables represented in the TMYe, temperature and humidity show very significant changes in current climatic trends, compared to radiation and wind speed. Moreover, while  $G_h$  is practically the same in TMYe and IWEC, the wind speed variable for TMYe is approximately half that of IWEC. This highlights the relevance of this variable at the microclimatic level, although its variations might not be as crucial for future scenarios, as there is hardly any variability among SSPs and years.

It is noteworthy that studying seasonal climate variability significantly helps in quantifying current and future climate behaviour. Likewise, it is crucial to consider not only mean values but also their variability in studies, especially in future scenarios. For instance, in the case of  $T_a$ , in addition to clear average differences between summer and winter, the annual interquartile ranges in 2050 are very similar, unlike those shown both annually and seasonally in 2080. Related to this idea, the selected indicators for the study, despite being simple methods, prove very interesting as they allow for the quantification of these fluctuations. Conversely, for a more exhaustive analysis of thermal comfort and building energy demand, it would be necessary to use other methodologies that consider the physical reactions of individuals, as well as urban, morphological, and building factors (Garshasbi et al., 2020).

## IV. CONCLUSIONS

The present methodology provides a robust estimation of climate evolution and the climatic, urban, and building-level impacts of climate change.

Among the main conclusions of this study is the generation and processing of a climate database, with over 10 years of records, which enabled the creation of an experimental Typical Meteorological Year (TMYe) for Madrid, using UNE-15927-4:2011. This TMYe shows annual mean values of outdoor air temperature ( $T_a$ ) of 16.0°C, relative humidity (RH) of 53%,

global horizontal solar radiation (Gh) of 386 W/m<sup>2</sup>, and wind velocity (Wv) of 1.39 m/s.

Compared to widely used climate files like IWEC, provided by EnergyPlus for Madrid, the TMYe better reflects current climate evolution. This is because its calculation is based on updated variables and an urban context within the city. Consequently, the TMYe indicates a climate that is 1.7°C warmer and 3 percentage points drier than IWEC, with slightly higher radiation (7 W/m<sup>2</sup>) and a clear reduction in wind intensity of 1.4 m/s. This trend is more evident in summer, with TMYe mean values of 25.8°C for Ta, 33% for RH, 494 W/m<sup>2</sup> for Gh, and 1.5 m/s for Wv. This trend is slightly discernible in spring and autumn, but less pronounced in winter.

Shared Socioeconomic Pathways (SSPs), which consider both climatic and socioeconomic factors, were used for the future climatic quantification of the TMYe. For this purpose, the Future Weather Generator tool, based on the "morphing" modelling of SSP1 to SSP5 scenarios and projections for 2050 and 2080, was applied.

From the study of climatic projections, it is concluded that as SSPs present greater challenges, Ta is clearly higher, while RH, Gh, and Wv do not appear to be as significantly impacted. Annually, these values are around 18°C, 51%, 402 W/m<sup>2</sup>, and 1.39 m/s for 2050. However, for the 2080 projection, these figures vary from 18.4°C to 20.41°C for Ta, and from 51% to 48% for RH in SSP1 to SSP5 scenarios, respectively. Conversely, the annual values of Gh and Wv are very similar, around 408 W/m<sup>2</sup> and 1.38 m/s. Notably, high temperatures and low humidity are obtained for the summer months, with seasonal averages of 28.8°C and 30% in 2050, potentially reaching 32.4°C and 26% in 2080 for SSP5.

Furthermore, to understand the implications of these meteorological variables, various indices were employed. At the climatic level, the TMYe file shows a notable decrease in the Extreme Temperature Range (ETR) compared to IWEC; however, it presents a higher number of Tropical Nights (TR) and Summer Days (SU), while Frost Days (FD) are significantly lower. For TMYe, ETR is 19°C, with similar values in SSPs for 2050 and around 20°C in 2080. The number of TR and SU for IWEC is 40 and 125, respectively. In the 2050 projection, these figures increase to 82 and 163 days, continuing their rise in 2080, reaching maximums of 108 TR and 186 SU in the 2080 scenario. It is very noticeable that this increase is largely due to data obtained not only in summer but also in spring and autumn. Finally, FD shows values similar to TMYe in 2050, and in 2080 they decrease until frost days disappear in SSP5.

In the analysis of outdoor thermal comfort, the TMYe file shows slightly higher outdoor heat discomfort values than the IWEC climate (annual values of 17% and 14% respectively). Climate projections indicate that thermal discomfort will increase in the future, reaching an annual level of 26% in 2050 and 32% in 2080. Moreover, in summer, it will increase to 77% and 85% for 2050 and 2080, showing intensities where most of the population suffers from heat discomfort. It is important to highlight that thermal discomfort will also be present in spring and autumn, with significant increases projected for 2050 and

2080.

Building energy demand indicators reveal that, compared to IWEC, TMYe shows lower heating degree-hours (HDD) and higher cooling degree-hours (CDD). The total HDD-CDD proportion is 95-5% for TMYe and 92-8% for IWEC, respectively. In the future, this trend is expected to continue; by 2050, a 13% decrease in HDD is projected, and CDD would increase by up to 225%. By 2080, HDD would reduce even further, and CDD would increase by up to 336%, with both cases including contributions from spring, which could account for up to 11% in 2080.

Finally, it is important to emphasize that the values obtained for SSP5 scenarios in 2050 are, in all cases, very similar to those shown for SSP1 in 2080. This indicates that inaction in implementing fair and accessible policies to limit current climatic trends could accelerate the effects of climate change by 30 years. To address this situation, the findings derived from this research serve as a basis for fostering adapted climate change mitigation plans, grounded in urban resilience, energy rehabilitation, and sustainable development. Therefore, the obtained results can be very useful for stakeholders involved in climate-responsible design and sustainable urban development.

#### ACKNOWLEDGEMENTS

The authors extend their gratitude to the funding entities of this work: The State Research Agency through the In-Situ-BEPAMAS project (Ref. PID2019-105046RB-I00/MICIN/AEI/10.13039/501100011033); and the URBAN-TherCOM research project PID2020-114873RA-C33. Additionally, the authors wish to acknowledge the European research project CO2NSTRUCT (Grant agreement ID: 101056862) funded by the European Commission under its Horizon Europe program.

#### REFERENCES

- AEMET. (2023). *Informe del estado del clima en España en 2022*, Agencia Estatal de Meteorología Española. <https://doi.org/10.31978/666-23-003-8>
- AENOR. (2011). *UNE-EN ISO-15927-4:2011*. www.aenor.es Tel.:902 Fax:913
- Amin, S., Giancola, E., Soutullo, S., Zorzalejo, L., & Em-, R. (2023). Evaluating the Impact of Climate Change & UHI on Energy Demand of a vulnerable neighborhood in Madrid. *5th Euro-Mediterranean Conference for Environmental Integration (EMCEI)*.
- ASHRAE. (2017). ANSI/ASHRAE Standard 55-2017: Thermal Environmental Conditions for Human Occupancy. *ASHRAE Inc.*, 2017, 66.
- Beck, H. E., Zimmermann, N. E., McVicar, T. R., Vergopolan, N., Berg, A., & Wood, E. F. (2018). Present and future köppen-geiger climate classification maps at 1-km resolution. *Scientific Data*, 5. <https://doi.org/10.1038/sdata.2018.214>
- Bianchi, C., & Smith, A. D. (2019). Localized Actual Meteorological Year File Creator (LAF): A tool for using locally observed weather data in building energy

- simulations. *SoftwareX*, 10. <https://doi.org/10.1016/j.softx.2019.100299>
- BOE 12925. (2022). *Real Decreto-ley 14/2022, de 1 de agosto, de medidas de sostenibilidad económica en el ámbito del transporte, en materia de becas y ayudas al estudio, así como de medidas de ahorro, eficiencia energética y de reducción de la dependencia energética del gas natural*. <https://www.boe.es/buscar/act.php?id=BOE-A-2022-12925>
- BOE 15820. (2007). *Real Decreto 1027/2007, de 20 de julio, por el que se aprueba el Reglamento de Instalaciones Térmicas en los Edificios*. <https://www.boe.es/buscar/act.php?id=BOE-A-2007-15820>
- Burillo, D., Chester, M. V., Pincetl, S., Fournier, E. D., & Reyna, J. (2019). Forecasting peak electricity demand for Los Angeles considering higher air temperatures due to climate change. *Applied Energy*, 236(July 2018), 1–9. <https://doi.org/10.1016/j.apenergy.2018.11.039>
- Castro Medina, D., Guerrero Delgado, Mc. C., Sánchez Ramos, J., Palomo Amores, T., Romero Rodríguez, L., & Álvarez Domínguez, S. (2024). Empowering urban climate resilience and adaptation: Crowdsourcing weather citizen stations-enhanced temperature prediction. *Sustainable Cities and Society*, 101. <https://doi.org/10.1016/j.scs.2024.105208>
- CTE. (2015). Índice Objeto Clima de referencia Climas de referencia en soporte informático (MET). *Código Técnico de La Edificación (Spain)*, 1–7.
- Database - Eurostat. (n.d.). Retrieved May 7, 2020, from <https://ec.europa.eu/eurostat/data/database>
- De Munck, C., Pigeon, G., Masson, V., Meunier, F., Bousquet, P., Tréméac, B., Merchat, M., Poeuf, P., & Marchadier, C. (2013). How much can air conditioning increase air temperatures for a city like Paris, France? *International Journal of Climatology*, 33(1), 210–227. <https://doi.org/10.1002/joc.3415>
- Díaz-López, C., Jódar, J., Verichev, K., Rodríguez, M. L., Carpio, M., & Zamorano, M. (2021). Dynamics of changes in climate zones and building energy demand. A case study in Spain. *Applied Sciences (Switzerland)*, 11(9). <https://doi.org/10.3390/app11094261>
- Eames, M., Kershaw, T., & Coley, D. (2012). A comparison of future weather created from morphed observed weather and created by a weather generator. *Building and Environment*, 56, 252–264. <https://doi.org/10.1016/j.buildenv.2012.03.006>
- Elnagar, E., Gendebien, S., Georges, E., Berardi, U., Doutreloup, S., & Lemort, V. (2023). Framework to assess climate change impact on heating and cooling energy demands in building stock: A case study of Belgium in 2050 and 2100. *Energy and Buildings*, 298. <https://doi.org/10.1016/j.enbuild.2023.113547>
- EnergyPlus. (n.d.). *Weather Data Sources | EnergyPlus*. Retrieved August 30, 2020, from <https://energyplus.net/weather/sources>
- Eurowho. (2021, December 9). *Heat threatens health: key figures for Europe*. World Health Organization. <https://www.euro.who.int/en/health-topics/environment-and-health/Climate-change/archive/heat-threatens-health-key-figures-for-europe>
- Finkelstein, J. M., & Schafer, R. E. (1971). Biometrika Trust Improved Goodness-Of-Fit Tests. In *Source: Biometrika* (Vol. 58, Issue 3). <http://www.jstor.orgURL:http://www.jstor.org/stable/2334400>
- Gangoellets, M., & Casals, M. (2012). Resilience to increasing temperatures: Residential building stock adaptation through codes and standards. *Building Research and Information*, 40(6), 645–664. <https://doi.org/10.1080/09613218.2012.698069>
- Garshasbi, S., Haddad, S., Paolini, R., Santamouris, M., Papangelis, G., Dandou, A., Methymaki, G., Portalakis, P., & Tombrou, M. (2020). Urban mitigation and building adaptation to minimize the future cooling energy needs. *Solar Energy*, 204, 708–719. <https://doi.org/10.1016/j.solener.2020.04.089>
- Giannakopoulos, C., Le Sager, P., Bindi, M., Moriondo, M., Kostopoulou, E., & Goodess, C. M. (2009). Climatic changes and associated impacts in the Mediterranean resulting from a 2 °C global warming. *Global and Planetary Change*, 68(3), 209–224. <https://doi.org/10.1016/j.gloplacha.2009.06.001>
- Herrera, M., Natarajan, S., Coley, D., Kershaw, T., Ramallo-González, A., Eames, M., Fosas, D., & Wood, M. (2017). A Review of Current and Future Weather Data for Building Simulation. *Building Services Engineering Research and Technology*, 38. <https://doi.org/10.1177/0143624417705937>
- ILO. (2019). Working on a warmer planet. The impact of heat stress on labour productivity and decent work. *International Labour Office*.
- International Energy Agency. (2017). Energy Technology Perspectives 2017 - Executive Summary. In *International Energy Agency (IEA) Publications*.
- IPCC. (2018). International Panel of Climate Change, 2018: Global Warming of 1.5°C. *United Union*.
- IPCC. (2021). Climate Change 2021: The Physical Science Basis. Contribution of Working Group I to the Sixth Assessment Report of the Intergovernmental Panel on Climate Change. In *Cambridge University Press* (Issue In Press).
- IPCC. (2022). *Climate Change 2022: Impacts, Adaptation, and Vulnerability. Contribution of Working Group II to the Sixth Assessment Report of the Intergovernmental Panel on Climate Change*.
- Jentsch, M. F., James, P. A. B., Bourikas, L., & Bahaj, A. B. S. (2013). Transforming existing weather data for worldwide locations to enable energy and building performance simulation under future climates. *Renewable Energy*, 55, 514–524. <https://doi.org/10.1016/j.renene.2012.12.049>
- Kalamees, T., Jylhä, K., Tietäväinen, H., Jokisalo, J., Ilomets,

- S., Hyvönen, R., & Saku, S. (2012). Development of weighting factors for climate variables for selecting the energy reference year according to the en ISO 15927-4 standard. *Energy and Buildings*, 47, 53–60. <https://doi.org/10.1016/j.enbuild.2011.11.031>
- Kan, X., Reichenberg, L., & Hedenus, F. (2021). The impacts of the electricity demand pattern on electricity system cost and the electricity supply mix: A comprehensive modeling analysis for Europe. *Energy*, 235. <https://doi.org/10.1016/j.energy.2021.121329>
- Lai, D., Lian, Z., Liu, W., Guo, C., Liu, W., Liu, K., & Chen, Q. (2020). A comprehensive review of thermal comfort studies in urban open spaces. In *Science of the Total Environment* (Vol. 742). Elsevier B.V. <https://doi.org/10.1016/j.scitotenv.2020.140092>
- Liu, Z., Li, J., & Xi, T. (2023). A Review of Thermal Comfort Evaluation and Improvement in Urban Outdoor Spaces. In *Buildings* (Vol. 13, Issue 12). Multidisciplinary Digital Publishing Institute (MDPI). <https://doi.org/10.3390/buildings13123050>
- López-Bueno, J. A., Díaz, J., Sánchez-Guevara, C., Sánchez-Martínez, G., Franco, M., Gullón, P., Núñez Peiró, M., Valero, I., & Linares, C. (2020). The impact of heat waves on daily mortality in districts in Madrid: The effect of sociodemographic factors. *Environmental Research*, 190(June). <https://doi.org/10.1016/j.envres.2020.109993>
- López-Moreno, H., Giancola, E., Sánchez Egido, M. N., Ferrer Tevar, J. A., & Soutullo Castro, S. (2021). *Evaluation of weather conditions in urban climate studies over different Madrid neighbourhoods: Influence of urban morphologies on the microclimate.* 1–12. <https://doi.org/10.18086/eurosun.2020.09.03>
- López-Moreno, H., Giancola, E., Sánchez Egido, M. N., & Soutullo Castro, S. (2022). Response of thermal comfort standards' applied to representative building typologies under new climate trends in Madrid. In *Innovación Tecnológica y Desarrollo Sostenible en la Edificación. Dykinson.*
- López-Moreno, H., Silvia, S., Sánchez, M. N., Emanuela, G., Javier, N. F., & Antonio, F. J. (2020). Outdoor thermal comfort approach in summer season for the city of Madrid. *PLEA 2020 Congress.*
- Martinopoulos, G., Alexandru, A., & Papakostas, K. T. (2019). Mapping temperature variation and degree-days in metropolitan areas with publicly available sensors. *Urban Climate*, 28. <https://doi.org/10.1016/j.uclim.2019.100464>
- Meyer, R. K. P. and L. A. (2014). *IPCC, 2014: Climate Change 2014: Synthesis Report* (Vol. 9781107025). <https://doi.org/10.1017/CBO9781139177245.003>
- MITECO. (2020). *Plan Nacional de Adaptación al Cambio Climático 2021-2030. España. Ministerio para la Transición Ecológica y el Reto Demográfico.* Ministerio para la Transición Ecológica y el Reto Demográfico.
- MSSSI. (n.d.). *Impacts on Health of Climate Change Executive summary, 2013. Informes, estudios e investigación Ministerio de sanidad, servicios sociales e igualdad.*
- Olmedo, R., Sánchez, M. N., Enriquez, R., Jiménez, M. J., & Heras María, R. (2016). *ARFRISOL Buildings-UIE3-CIEMAT. In: Janssens A, editor. Report of Subtask 1a: Inventory of full scale test facilities for evaluation of building energy performances. IEA EBC Annex 58.* www.ugent.be
- OrtizBeviá, M. J., Sánchez-López, G., Alvarez-García, F. J., & RuizdeElvira, A. (2012). Evolution of heating and cooling degree-days in Spain: Trends and interannual variability. *Global and Planetary Change*, 92–93, 236–247. <https://doi.org/10.1016/j.gloplacha.2012.05.023>
- Palme, M., & Salvati, A. (2021). Urban Microclimate Modelling for Comfort and Energy Studies. *Urban Microclimate Modelling for Comfort and Energy Studies.* <https://doi.org/10.1007/978-3-030-65421-4>
- Pérez-Andreu, V., Aparicio-Fernández, C., Martínez-Ibernón, A., & Vivancos, J. L. (2018). Impact of climate change on heating and cooling energy demand in a residential building in a Mediterranean climate. *Energy*, 165, 63–74. <https://doi.org/10.1016/j.energy.2018.09.015>
- Programs, A. (2022). *EnergyPlus™ Version 22.1.0 Documentation.*
- Reiter, S. (2004). *Correspondences between the conception principles of sustainable public spaces and the criteria of outdoor comfort.*
- Rodrigues, E., Fernandes, M. S., & Carvalho, D. (2023). Future weather generator for building performance research: An open-source morphing tool and an application. *Building and Environment*, 233. <https://doi.org/10.1016/j.buildenv.2023.110104>
- Sánchez, M. N., Soutullo, S., Olmedo, R., Bravo, D., Castaño, S., & Jiménez, M. J. (2020). An experimental methodology to assess the climate impact on the energy performance of buildings: A ten-year evaluation in temperate and cold desert areas. *Applied Energy*, 264(February), 114730. <https://doi.org/10.1016/j.apenergy.2020.114730>
- Scortichini, M., de Sario, M., De'donato, F. K., Davoli, M., Michelozzi, P., & Stafoggia, M. (2018). Short-term effects of heat on mortality and effect modification by air pollution in 25 italian cities. *International Journal of Environmental Research and Public Health*, 15(8). <https://doi.org/10.3390/ijerph15081771>
- Sirombo, E., Filippi, M., Catalano, A., & Sica, A. (2017). Building monitoring system in a large social housing intervention in Northern Italy. *Energy Procedia*, 140, 386–397. <https://doi.org/10.1016/j.egypro.2017.11.151>
- Soutullo, S., Giancola, E., Jiménez, M. J., Ferrer, J. A., & Sánchez, M. N. (2020). How climate trends impact on the thermal performance of a typical residential building in Madrid. *Energies*, 13(1). <https://doi.org/10.3390/en13010237>
- Thom, E. C. (1959). The Discomfort Index. *Weatherwise*, 12(2), 57–61. <https://doi.org/10.1080/00431672.1959.9926960>
- Tselepidaki, I., Santamouris, M., Moustris, C., & Pouloupoulou, G. (1992). Analysis of the summer discomfort index in Athens, Greece, for cooling purposes. In *Energy and Buildings* (Vol. 18).

- Weir, E. (2002). Heat wave: first, protect the vulnerable. *CMAJ: Canadian Medical Association Journal = Journal de l'Association Médicale Canadienne*, 167(2), 169.
- WMO-No. 8. (2012). *Guide to Instruments and Methods of Observation* | World Meteorological Organization. [https://community.wmo.int/en/activity-areas/imop/wmo-no\\_8](https://community.wmo.int/en/activity-areas/imop/wmo-no_8)



**Reconocimiento – NoComercial (by-nc):** Se permite la generación de obras derivadas siempre que no se haga un uso comercial. Tampoco se puede utilizar la obra original con finalidades comerciales.